Uludağ University Journal of The Faculty of Engineering, Vol. 30, No. 3, 2025 RESEARCH

DOI: 10.17482/uumfd.1767600

COMPARISON OF OCTAGONAL AND TWISTED FINS FOR BATTERY THERMAL MANAGEMENT IN UNMANNED AERIAL VEHICLES AT HIGH DISCHARGE RATES

Onur YAŞAR [*]

Received: 20.08.2025 ; revised: 07.10.2025 ; accepted: 29.10.2025

Abstract: Cooling strategy including fins is considered as an effective approach due to its successful results, especially in batteries. To maintain the battery peak temperature within a desired range and thereby improve flight performance and extend service life of unmanned aerial vehicles (UAVs), this paper deals with fin cooling of lithium-polymer batteries. A 6s1p lithium-polymer battery is modeled with octagonal and twisted fins separately. Both models are simulated in a wind tunnel by using RNG k-ε model. Peak temperatures of finless battery model are compared with those of finned models. The motivation of this study is to improve flight performance and extend service life of UAVs by ensuring thermal management of pouch-type lithium-polymer batteries under high discharge rates using octagonal and twisted fins. According to the results, battery model including twisted fins enables lower peak temperatures approximately by 1 K compared to those of octagonal fins under the same boundary conditions. Inlet air temperature of 268.15 K and inlet air velocity of 2.4 m/s for battery models with octagonal and twisted fins can keep peak temperature at 307.44 K and 305.97 K, respectively. This paper provides an insight into the significance of novel fins for battery thermal management in UAVs.

Keywords: Discharge rate, Thermal management, Battery, Temperature

Yüksek Deşarj Oranlarında İnsansız Hava Araçlarında Batarya Isıl Yönetimi İçin Sekizgen ve Bükümlü Kanatçıkların Karşılaştırılması

Öz: Kanatçıklı soğutma yöntemi, özellikle bataryalarda başarılı sonuçları nedeniyle, etkili bir yaklaşım olarak kabul edilmektedir. Batarya tepe sıcaklığını istenen aralıkta tutmak ve böylece insansız hava araçlarının (İHA) uçuş performansını iyileştirmek ve servis ömrünü uzatmak için, bu makale lityum-polimer bataryaların kanatçık ile soğutmasını ele almaktadır. Bir 6s1p lityum-polimer batarya, sekizgen ve bükülmüş kanatçıklarla ayrı ayrı modellenmiştir. Her iki model de bir rüzgar tünelinde RNG k-ε modeli kullanılarak simüle edilmiştir. Kanatçıksız batarya modelinin tepe sıcaklıkları, kanatçıklı modellerin tepe sıcaklıkları ile karşılaştırılmıştır. Bu çalışmanın motivasyonu, sekizgen ve bükülmüş kanatçıkları kullanarak yüksek deşarj oranlarında kese tipi lityum-polimer bataryaların ısıl yönetimini sağlamak suretiyle İHA'ların uçuş performansını artırmak ve servis ömrünü uzatmaktır. Sonuçlara göre, bükülmüş kanatçıkları içeren batarya modeli, aynı sınır şartları altında sekizgen kanatçıklara kıyasla yaklaşık 1 K daha düşük tepe sıcaklıklarına olanak sağlamaktadır. Sekizgen ve bükülmüş kanatçıklı batarya modelleri için 268.15 K hava giriş sıcaklığı ve 2.4 m/s hava giriş hızı, tepe sıcaklığını sırasıyla 307.44 K ve 305.97 K'de tutabilmektedir. Bu çalışma, İHA'larda batarya ısıl yönetimi için yeni kanatçıkların önemine dair bir bakış açısı sunmaktadır.

Anahtar Kelimeler: Deşarj oranı, Isıl yönetim, Batarya, Sıcaklık

[*] Balıkesir University, Faculty of Engineering, Department of Mechanical Engineering,10463, Balıkesir, Türkiye

Corresponding Author: Onur Yaşar (onur.yasar@balikesir.edu.tr)

1. INTRODUCTION

Lithium-polymer batteries are common batteries providing high energy densities and rechargeable feature, especially at high discharge rates in unmanned aerial vehicles or electric vehicles (Sefkat and Ozel, 2020; Bhawna et al., 2025). During high discharge rates, considerable volumetric heat is generated (Tan et al., 2025). It is related to current and voltage of battery, which can result in excessive internal temperature rise (Sutheesh et al., 2024). Decreasing cell temperature below 35°C is advantageous for both battery and system operations, especially for UAVs in terms of service life and flight performance (Schimpe et al., 2018; Li et al., 2021). Therefore, temperature prediction is significant at lithium-polymer batteries (Li et al., 2021). In order to predict maximum cell temperature, computational fluid dynamics (CFD) is useful tool (Cui et al., 2025). In CFD simulations, fin-based cooling systems are employed. Aluminum fins, enabling high thermal conductivity, are suggested (Aslan et al., 2022).

There are numerous studies about battery thermal management using fins. Hence, Li et al. (2024) suggested a cold plate with offset fins to cool a 40Ah prismatic lithium battery module. Thermal and hydraulic performance of proposed system is investigated by using CFD simulations. Analyzes are validated against previous studies. The results indicate that overall maximum temperature decreases to nearly 45°C. Average error between CFD simulations and previous studies is about 5%. Akula et al. (2024) proposed PCM-fin cooling structure for 18650 lithium-ion batteries. In the study, fin configurations ranging between two plate fins and 390 pin fins are utilized to examine temperature gradients at 3C, 4C and 5C discharge rates. CFD simulations are performed to reveal battery temperatures. At the end of the study, it is stated that 260 fins can be suggested at 5C discharge rate from the viewpoint of weight and thermal performance.

Luo et al. (2024) utilized snowflake fins, a liquid cooling strategy, and PCM to cool 26650 $LiFePO_4$ batteries at 3C and 5C discharge rates. Temperature distributions of thermal management system are studied by conducting simulations validated against previous studies from open literature. According to the results, snowflake fins decrease peak temperature of batteries below 318 K at 3C discharge rate, while battery peak temperature is much higher at 5C discharge rate and 40°C ambient temperature conditions. Recent studies focus attention on battery thermal management by utilizing A-shaped, V-shaped fins, honeycomb-like fins or liquid cooling plates. Ismail et al. (2025) employed PCM, A-shaped and V-shaped fins for thermal management of lithium-ion batteries. Fins are placed in horizontal or vertical configuration with different numbers and angles under 5C discharge rate to investigate cell temperature during melting and solidification process of PCM. According to results, the best performance is achieved with 7 and 9 horizontal fins at 720 s and 480 s, respectively. These configurations decrease cell temperature to 42.5°C and 38.3°C, respectively. Fu et al. (2025) used a cooling plate integrated with honeycomb-like fins to cool a 55 Ah pouch lithium-ion battery by performing CFD analyzes. Simulations are carried out at discharge rates of 0.7, 1.0, and 1.2 C and validated against experiments. It is asserted that maximum cell temperature can be maintained at approximately 28°C by using orthogonally optimized scheme. Zhang et al. (2025) focused attention on battery thermal management systems both experimentally and numerically by using liquid cooling plates integrated with cavities and fins. Six different fin structures, including diamond, shuttle, droplet, rectangular, circular, and triangular, are utilized to cool battery systems. The results exhibit that droplet-shaped fins provide the lowest temperatures of approximately by 26°C. Different studies from open literature are presented in Table 1.

Table 1. Literature review

Citation	Heat Sink/Battery	Battery Shape	Fluid	Cooling Method	Discharge Rate	Baseline Fin Shape	Inlet Air Temperature	Maximum Temperature
Ghalambaz et al. (2021)	Heat Storage System	Not Available	Water	PCM and fin cooling	Not Available	Twisted fin array	323.15 K (for hot water)	approximately 325 K
Sun et al. (2021)	Energy storage system	Not Available	Water	PCM and fin cooling	Not Available	Twisted fins	283.15 K, 288.15 K and 293.15 K (for hot water)	approximately 324 K (PCM average temperature)
Bo et al. (2022)	Thermal energy storage system	Not Available	Water	PCM and fin cooling	Not Available	Twisted fins array	288 K (for hot water)	approximately 363 K (PCM average temperature)
Liu et al. (2022)	Battery	Cylindrical	Air	PCM and fin cooling	1C, 2C and 3C	Spiral fins	Not Available	approximately 356 K (for 3C discharge rate without PCM) & approximately 313 K (with spiral fins)
Fan et al. (2023)	Battery	Prismatic	Not Available	Bionic fishbone channel liquid cooling plate	5C and 6C	Not Available	298.15 K (initial inlet coolant temperature)	approximately 309 K
Xiong et al. (2023)	Battery	Pouch	Water	Fin cooling	5C	Circular, equilateral triangular, square and elliptical	298.15 K (starting temperature of liquid)	306 K
Zhao et al. (2023)	Battery	Cylindrical	Air	Different battery configurations	0.5C, 1C and 2C	Not Available	293.15 K	329 K (for design 1, the flow rate is 11.88 L/s)
Pan et al. (2023)	Heat Sink	Not Available	Not Available	Fin and PCM cooling	Not Available	Circle, triangle-p, triangle-i, square, pentagon-p, pentagon-i, hexagon and octagon fins	Not Available	approximately 324 K
Dagdevir and Ding (2024)	Battery	Cylindrical	Air	PCM and fin cooling	1C, 2C, 3C and 4C	Helical fins	Not Available	approximately 335 K (for 4C discharge rate)
Alzwayi and Paul (2024)	Battery	Cylindrical	Air	Fin cooling	1C, 1.5C, 2C and 2.5C	Vertical and spiral fins	Not Available	approximately 321 K (for 2.5 C discharge rate without fins)

The originality of this work lies in the investigation of peak temperature values of a pouch type 6s1p lithium-polymer battery at a high discharge rate to improve flight performance and extend service life of unmanned aerial vehicles (UAVs), using octagonal and twisted fins, which are different from those of employed in previous studies. The major difference of this paper is to fill the gap of literature by using both octagonal and twisted fins under forced convection

conditions at 6C discharge rate for lithium-polymer batteries. The 6s1p battery model in wind tunnel is simulated at 6C discharge rate using ANSYS Fluent software. Peak temperature values of battery models with octagonal and twisted fins at different inlet velocities and temperatures are highlighted and compared with those of the finless model. Authors claim that this study will be a benchmark for future studies to be utilized and validated in the literature.

2. CFD METHOD

2.1. Mathematical Approach and Boundary Conditions

Mathematical approach of fluid domain is described using incompressible Navier-Stokes equations (Cheng et al., 2020). These equations are used to solve the fluid motion for both fluid and gas phases. Main equations are continuity and momentum equations, which are expressed as follows (Chen et al., 2019).

$$\nabla.\vec{V} = 0 \tag{1}$$

$$\rho.\frac{D\vec{V}}{Dt} = -\nabla P + \mu.\nabla^2.\vec{V} + \rho\vec{g} \tag{2}$$

Eqs. 1 and 2 indicate that $\vec{V}$, ρ, P, g are velocity, density, pressure and gravitational acceleration, respectively. In addition to these terms, t and μ signify time and dynamic viscosity, respectively. These terms are utilized to solve both laminar and turbulent flows (Chen et al., 2020). Since solving the Navier Stokes equations is difficult, turbulence models are preferred. The RNG (Renormalization Group) k-ε model provides accurate solutions in wind tunnel analyses (Li et al., 2013). Compared to standard k-ε model, RNG k-ε model requires more computational time. Main equation of RNG k-ε model is as follows (Yakhot et al., 1992).

$$\frac{\partial}{\partial t}(\rho\varepsilon) + \frac{\partial}{\partial x_i}(\rho\varepsilon u_i) = \frac{\partial}{\partial x_j}\left(\alpha.\varepsilon\mu_{eff}\frac{\partial_\varepsilon}{\partial x_j}\right) + C_{1\varepsilon}\frac{\varepsilon}{k}(G_k + C_{3\varepsilon}G_b) - C_{2\varepsilon}\rho\frac{\varepsilon^2}{k} + R_\varepsilon - S_\varepsilon \tag{3}$$

R and S are additional and source terms. R is related to turbulent strain effects. α, ε, k are Prandtl number, dissipation rate and kinetic energy, respectively (Perini et al., 2017). RNG k-ε model provides appropriate results in battery cooling simulations. Hence, all CFD simulations are carried out using this turbulence model (Li et al., 2013). Octagonal geometry provides increased surface area (Murthy et al., 2024). On the other hand, twisted fins enable higher heat transfer coefficient and uniform temperature distribution (Ji et al., 2025). To date, both twisted and octagonal fins have not been used to battery cooling in a wind tunnel.

Boundary conditions represent interaction between fluid and environment, including pressure, velocity, and temperature for both inlet and outlet (Dönmez and Bulut, 2024). In this study, velocity inlet and pressure outlet conditions are adopted. Near tunnel walls, no-slip boundary condition is applied (Bhave and Taherian, 2014). Simulations are carried out in steady-state conditions with constant heat generation (Uzal et al., 2023). Inlet air velocities are selected as 1, 1.6, 2, 2.4 and 3 m/s to ensure the turbulent flow (Wang et al., 2025). Inlet air temperatures are set at 263.15 K, 268.15 K, 273.15 K and 278.15 K for efficient cooling. These inlet temperatures correspond to a flight altitude of approximately 2 to 4 kilometers in UAVs (Sissenwine et al., 1976; Cho et al., 2016). Second-Order Upwind Scheme is utilized for analyzes. For pressure-velocity coupling, SIMPLE algorithm is used (Wang et al., 2008). Volumetric heat generation equation is adopted to calculate heat generation rate. This equation also known as Bernardi equation is as follows (Bernardi et al., 1984).

$$\dot{Q} = I.\ (V\text{-}V_{oc}) - I.T.\frac{dV_{oc}}{dT} \quad (4)$$

where, V and I are primary electrical terms, voltage and current, respectively. Moreover, T and V_{oc} indicate temperature and open circuit voltage, which significantly affects the heat generation rate (Sefkat and Ozel, 2020; Vashisht et al., 2025). Simulations are performed at discharge rate of 6C. It corresponds to a heat generation rate of 142288 W/m^3. Therefore, severe thermal conditions are considered to evaluate cooling effectiveness of these fins (Fan et al., 2023). However, cell temperature is not only related to volumetric heat generation rate (Shi et al., 2025). Thermo-physical properties of battery model and fins as well as volumetric heat generation rate, affect cell temperature. These properties are density, specific heat capacity, and thermal conductivity, respectively (Emam and Ahmed, 2018; Esmaeili and Khoshvaght-Aliabadi, 2023). These properties can be seen in Table 2.

Table 2. Specifications of battery model, air and aluminum (Mahamud and Park, 2011; Esmaeili and Khoshvaght-Aliabadi, 2023; Aljumaili et al., 2024; Incropera and DeWitt, 2024).

Thermo-Physical Property	Battery Model	Air	Aluminum
Specific Heat Capacity (kJ/kg.K)	1.3	1.00643	0.093
Density (kg/m^3)	2100	1.225	2675
Thermal Conductivity (W/m.K)	22	0.0242	211

Table 2 clearly indicates that aluminum has a higher density and thermal conductivity than model material to decrease cell temperatures in simulations. The high thermal conductivity of aluminum enables dissipation of heat generated by the cells (Liu et al., 2023).

2.2. Descriptions of Battery Model and Wind Tunnel

The dimensions of battery model and fins are important parameters that affect cell temperatures. In this study, a 6s1p lithium-polymer battery is modeled based on its actual dimensions (Liu et al., 2023; ERCmarket Website, 2025). The main dimensions and properties of battery are given in Table 3.

Table 3. Specifications of lithium-polymer battery (ERCmarket Website, 2025).

Property	Explanation
Capacity (mAh)	5100
Voltage (V)	22.2
Weight (g)	760
Length (mm)	149
Width (mm)	50
Height (mm)	52

As seen in Table 3, the model has a rectangular prism shape, with each cell having a voltage of 3.7 V (ERCmarket Website, 2025). Dimensions of wind tunnel are considered based on size of battery model (Wang et al., 2016). Specifications of wind tunnel and battery model with boundary conditions are illustrated in below.

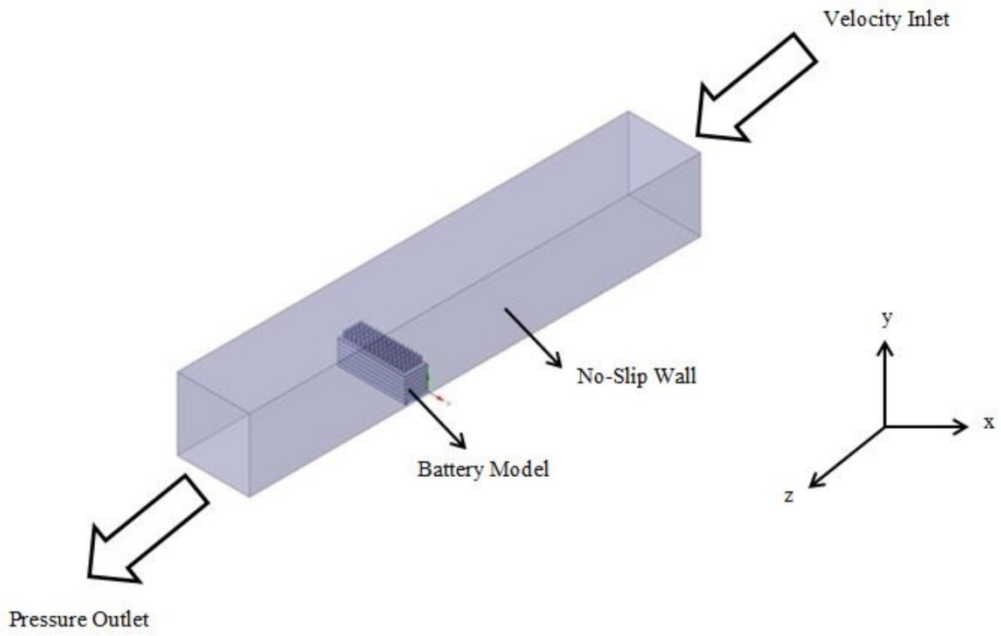

Fig. 1:
Illustration of simplified models of battery and wind tunnel with boundary conditions

As illustrated in Fig. 1, air direction is along the +z direction. The distance between battery model and tunnel outlet is more than 1 m. Octagonal and twisted fins are employed in simulations. Top-down view of fins can be seen in Fig. 2.

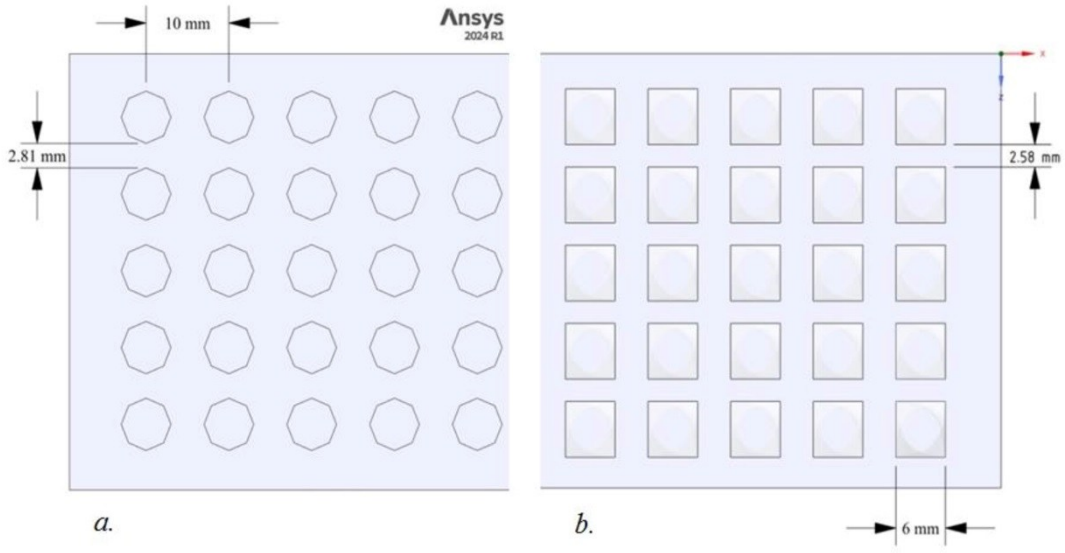

Fig. 2:
Top-down view of fins (a=Octagonal, b=Twisted)

According to Fig. 2, center-to-center spacing of octagonal fins is 10 mm horizontally. Corner-to-corner spacing of octagonal fins is 2.81 mm vertically. Fin length of octagonal fins is 2.29 mm. Edge-to-edge spacing of twisted fins is 2.58 mm vertically. Fin length of twisted fins is approximately 6 mm. Total number of fins is 70 for both models. Total heat transfer areas of

battery models with octagonal and twisted fins are calculated as 143375 mm^2 and 145625 mm^2, respectively.

2.3. Grid Generation

Grid generation using finite volume method can be required for system analysis (Sharma et al., 2021). In this method, analyzed system is divided into smaller elements that can be poly-hedral, tetrahedral or hexahedral (Kim et al., 2022; Yousefi et al., 2025). Among these element types, tetrahedral elements can be generated more easily (Kummitha, 2023). Generated mesh can be seen in Fig. 3.

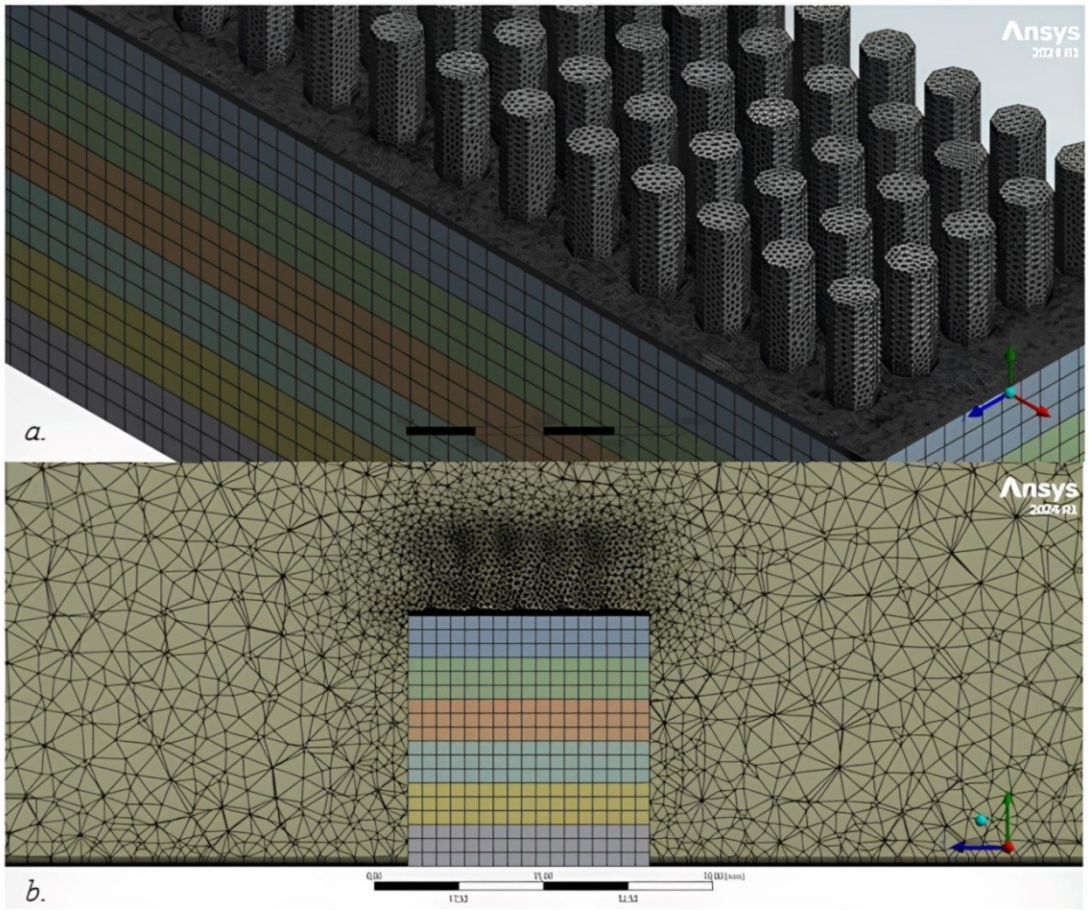

Fig. 3:
Generated mesh of battery model and flow domain (a=Battery, b=Flow domain)

According to Fig. 3, denser elements are used near the battery (Xiao et al., 2023; Yousefi et al., 2025). Ten inflation layers are employed to capture boundary layer effects, especially in turbulent flows (Sklavounos and Rigas, 2006). The first layer thickness of inflation layers is calculated by using the following formula (Shukla et al., 2012).

$$y^{+}= \left(\frac{u.y}{\upsilon}\right) \tag{5}$$

where, υ is kinematic viscosity of air. u signifies velocity. y is the distance of the first cell from the wall to ensure y^+ is less than 1. y^+ is dimensionless wall distance used in CFD simulations (Shukla et al., 2012; Li et al., 2013). Mesh sensivity analysis is an essential step in grid generation. It depends on effect of different element sizes on simulation results (Larrañaga-Ezeiza et al., 2022). This analysis is performed with different element sizes and number of elements corresponding to maximum cell temperatures (Lv et al., 2025). Grid independence test based on element size can be seen in Fig. 4.

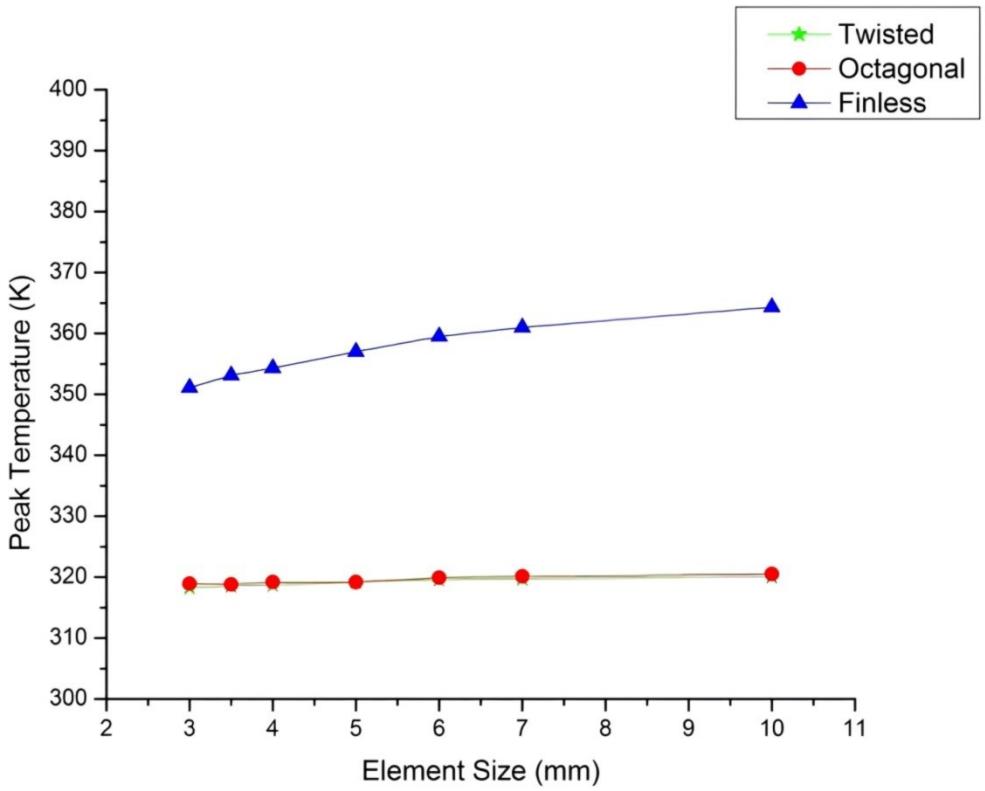

Fig. 4:
Grid independence test

Fig. 4 clearly indicates that maximum cell temperatures do not change considerably (Lv et al., 2025). Reliability of results is validated by performing grid generation with different element sizes. Element size of 4 mm is considered in simulations. In addition to element size, mesh quality is investigated. Mesh quality is evaluated with minimum orthogonal quality and maximum skewness values. Minimum orthogonal quality values for battery models with octagonal fins, twisted fins, and without fins are 0.23, 0.22 and 0.21, respectively. Maximum skewness values for these models are 0.76, 0.77 and 0.78, respectively, indicating proper mesh quality (Ansys, 2013; Adam et al., 2020).

3. RESULTS AND DISCUSSION

In this section, effect of inlet air velocity on maximum cell temperatures is examined graphically. The main objective of this paper is based on temperature distribution of battery models. Hence, the results are given only based on temperature results. Effect of inlet air velocity on maximum cell temperature at 263.15 K is seen in Fig. 5.

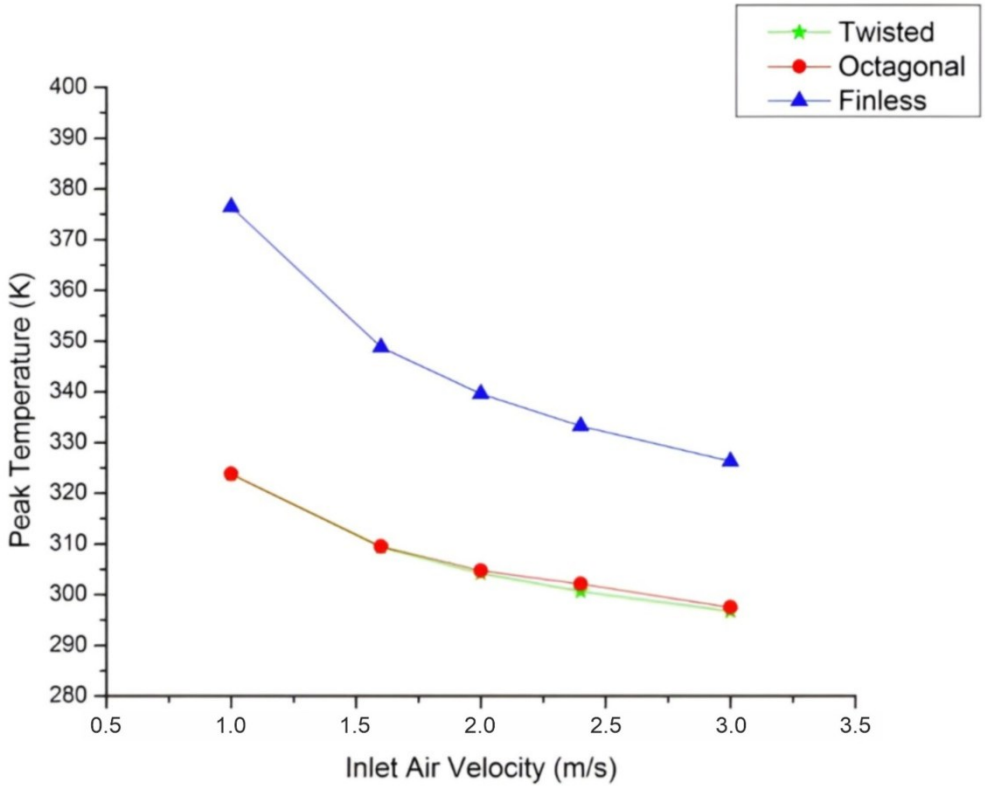

Fig. 5:
Effect of inlet air velocity on peak temperature of battery at 263.15 K

Fig. 5 clearly illustrates that peak temperature of battery model decreases gradually as inlet air velocity increases from 1 m/s to 3 m/s (Bamrah et al., 2022). Peak temperatures of battery models with octagonal and twisted fins at inlet air velocity of 1m/s and inlet air temperature of 263.15 K are 323.66 K and 323.80 K, respectively. Under the same boundary conditions, peak temperature of finless battery model is 376.46 K. As the inlet air velocity increases 1 m/s to 3 m/s, maximum cell temperature decreases by approximately 8% for both finned models. Effect of inlet air velocity on peak temperature of battery models at 268.15 K is presented in Fig. 6.

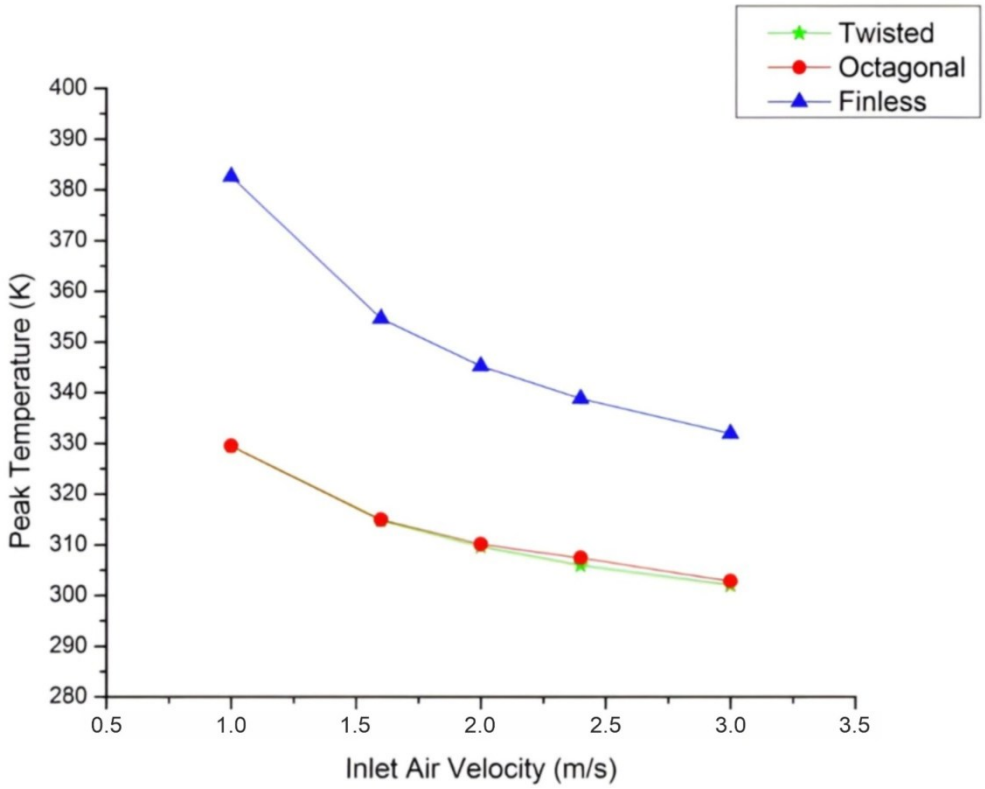

Fig. 6:
Effect of inlet air velocity on peak temperature of battery at 268.15 K

According to Fig. 6, peak temperatures of battery model with twisted fins are 329.4 K, 314.76 K, 309.61 K, 305.97 K and 302.01 K for inlet air velocity of 1, 1.6, 2, 2.4 and 3 m/s, respectively, which are slightly lower than those of octagonal fins. Twisted fins enable secondary flow enhancement and increased turbulence. Hence, they provide higher Nusselt number, heat transfer coefficient and better cooling performance (Ji et al., 2025). Maximum cell temperature decreases by approximately 4% as inlet air velocity increases from 1.6 m/s to 4 m/s. Even at inlet air velocity of 3 m/s, peak temperature of battery without fins is higher than 331 K. Inlet air temperature has a considerable effect on peak temperatures of battery models. Maximum temperature values obtained at inlet air temperatures of 263.15 K and 268.15 K fall within the acceptable range reported in Sun et al. (2021), Liu et al. (2022), Fan et al. (2023), Xiong et al. (2023) and Alzwayi and Paul (2024), which are listed in Table 1 (Bamrah et al., 2022; Patil et al., 2020). Peak temperature of finless model can exceed 385 K, which indicates a severe risk of battery fire. From the viewpoint of safe operating temperature of lithium batteries, peak temperature shouldn't exceed 308 K, which can be achieved with higher Reynolds numbers (Wang et al., 2019; Hasan et al., 2023). Effect of inlet air velocity on peak temperatures of battery models at 273.15 K is given in Figs. 7 and 8, respectively.

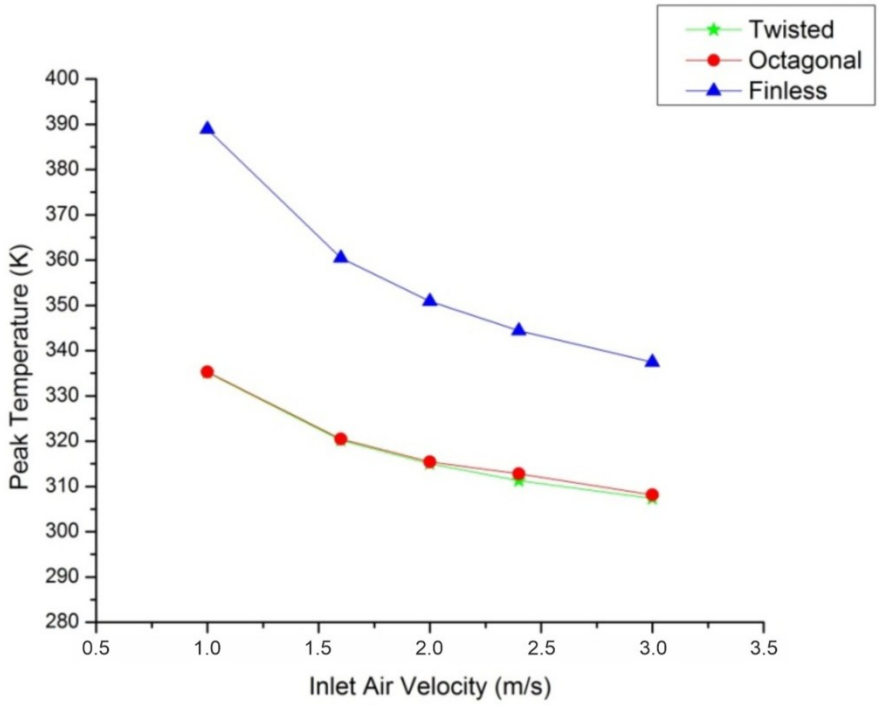

Fig. 7:
Effect of inlet air velocity on peak temperature of battery at 273.15 K

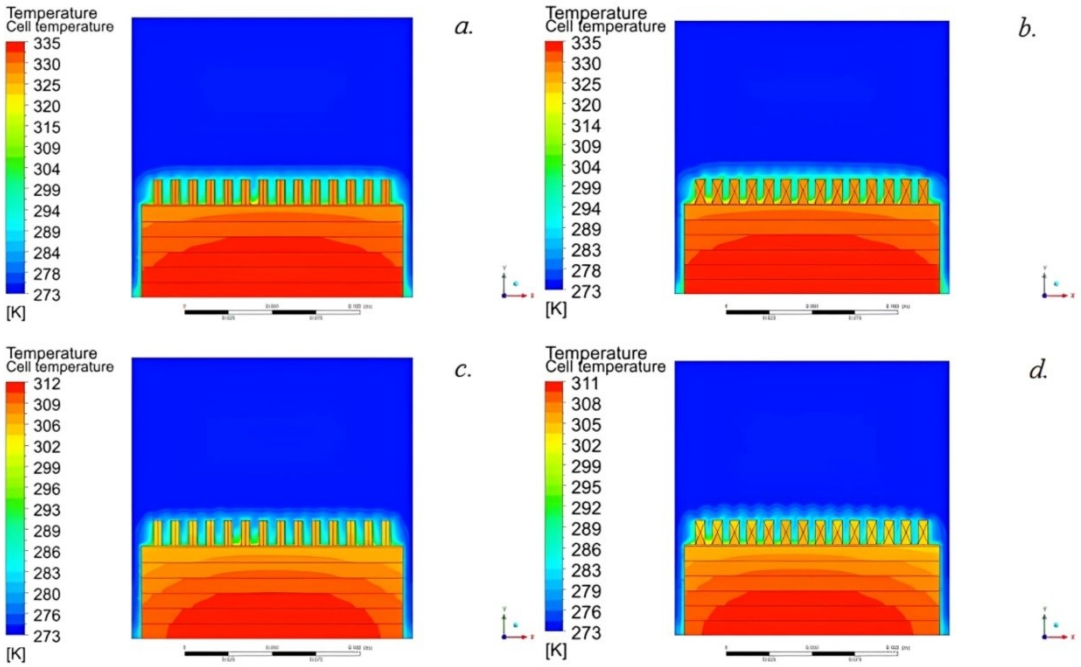

Fig. 8:
Temperature variation of battery at 273.15 K (a=Octagonal for 1 m/s, b=Twisted for 1 m/s, c=Octagonal for 2.4 m/s, d=Twisted for 2.4 m/s)

As evident in Figs 7 and 8, peak temperature of battery reduces to 311 K. Temperature difference of about 5 K is seen between the lowermost and uppermost cells, which is acceptable according to the literature (Zolot et al., 2002; Chen et al., 2016). Under same boundary conditions, octagonal fins yield 0.04–0.48% higher temperature compared to twisted fins. Maximum cell temperature decreases by approximately 1.5% between inlet air velocities of 1.6 m/s and 2 m/s. Peak temperatures of finned and finless models at inlet air velocity of 1 m/s and inlet air temperature of 278.15 K can be seen in Figs 9 and 10, respectively.

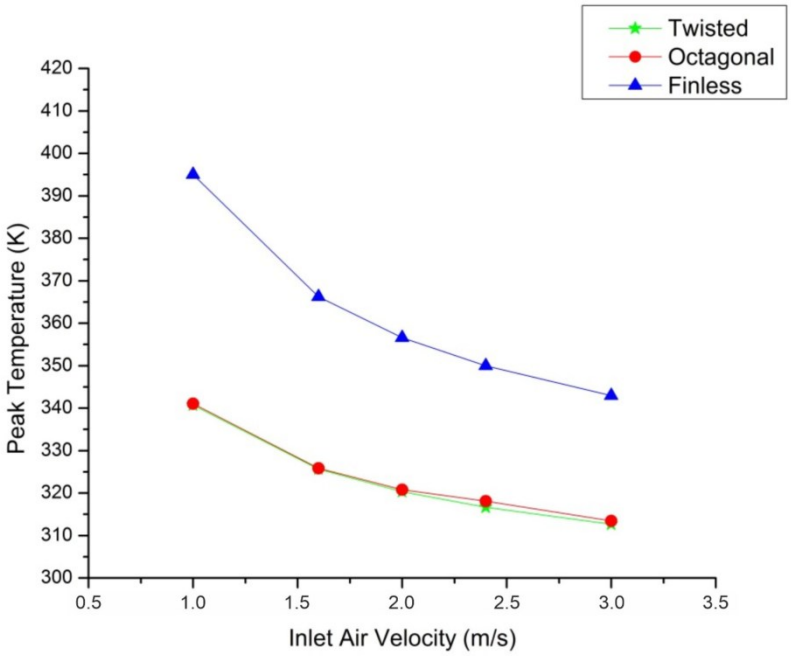

Fig. 9:
Effect of inlet air velocity on peak temperature of battery at 278.15 K

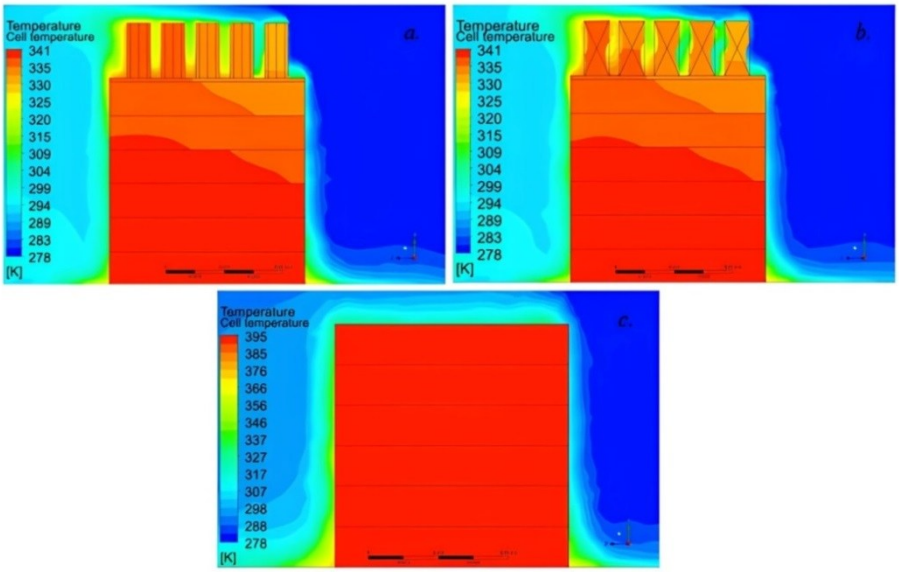

Fig. 10:
Peak temperatures of battery models at inlet air temperature of 278.15 K and inlet air velocity of 1 m/s (a=Octagonal, b=Twisted, c=Finless)

As indicated in Figs 9 and 10, peak temperatures of finned models are about 340 K, which are not recommended for lithium-polymer batteries. Under the same conditions, peak temperature of finless model is approximately by 390 K. Compared to finless model, finned models reduce maximum cell temperature by up to 14%. According to open literature, the initial stage of thermal runaway starts above 363.15 K. At this temperature, SEI layer decomposes. Moreover, separator breaks down at approximately 403.15 K. At higher temperature such as 473.15 K, electrolyte breaks down. The temperature reaches very high values, around 390 K in this manuscript. Therefore, this value corresponds to the temperature at which decomposition of SEI layer begins. It is explained in revised manuscript (Domalanta and Paraggua, 2023). Consequently, twisted fins used at high Reynolds numbers and low inlet temperatures are highly recommended for battery cooling, particularly at high discharge rates (Wang et al., 2019; Sun et al., 2021). This results in an improvement in flight performance and in service life of UAVs (Li et al., 2021). Longer service life is advantageous during high power-demanding phases such as landing and take-off (Li and Liu, 2022).

In the absence of experimental data, grid impendence analysis and different models are taken into account. Table 1 clearly indicates that the maximum temperature values obtained at inlet air temperatures of 263.15 K and 268.15 K are supported by the results of Sun et al. (2021), Liu et al. (2022), Pan et al. (2023) and Alzwayi and Paul (2024).

4. CONCLUSION

The main objective of this paper is to compare the cooling performance of octagonal and twisted fins under steady-state conditions for lithium-polymer batteries. Models of pouch type lithium-polymer battery with octagonal and twisted fins are utilized. The objective of this study is to keep battery temperature below 308 K and to determine which fin model provides lower temperatures in order to improve flight performance and extend service life of UAVs. The main findings are explained in below.

- Compared to octagonal fins, twisted fins provide lower temperatures, by approximately 1-2 K, under the same boundary conditions.
- For the same inlet air velocities and temperatures, 0.04–0.48 % lower temperatures are obtained with twisted fins compared to octagonal fins.
- In order to obtain peak temperatures below 35°C, inlet air temperatures of 263.15 K, 268.15 K with high Reynolds numbers are suggested.
- Battery peak temperature can be maintained below 308 K, even at 273.15 K of inlet air temperature and 3 m/s of inlet air velocity for twisted fins. However, peak temperature exceeds 308 K at 278.15 K of inlet air temperature.
- Temperature difference of about 5 K is seen between the lowermost and uppermost cells.
- Battery peak temperature without fins can exceed 380 K, which can result in thermal runaway of battery. This indicates the importance of fins for battery thermal management. Keeping battery peak temperature below 308 K may positively affect flight performance and service life of UAVs, especially during the landing and take-off phases.
- Under same boundary conditions, octagonal or twisted fins provide up to 14% lower cell temperatures compared to finless model.
- RNG k-ε model Enhanced Wall Treatment with mesh sensivity analyzes provide good results without validation.

Twisted and octagonal fins can be used for battery thermal management at high discharge rates based on these results. This paper will be completed by:

- Experimental setup or data should be used to carry out novel studies.
- In addition to fins, phase-change materials and metal foams can be used.
- 3C, 4C, 5C and 7C discharge rates can be utilized for comparison.
- Transient simulations with time-step independence analyzes can be performed.
- Time-dependent changes in current, voltage and depth-of-discharge can be obtained with the use of more realistic battery model.
- Different fin lengths, spacings, geometries, and heights are required for an extensive evaluation.
- Pressure drop, Nusselt number, heat transfer coefficient, velocity vectors and streamlines should be investigated for a deeper analysis.
- Uncertainty analysis is required for original studies.
- Oblong, lancet, piranha, stepped fins etc… can be used for battery thermal management.
- Different materials with higher thermal conductivity can be used.
- Lighter materials due to weight factor can be selected.
- These fin structures can be applied in larger UAVs at higher discharge rates.
- Metaheuristic algorithms and machine learning methods can be employed in addition to CFD analyzes.
- The verification of the results through both numerical simulations and experimental validations will contribute to the emergence of new industrial applications.

CONFLICT OF INTEREST

The author declares no conflicts of interest.

AUTHOR CONTRIBUTION

Onur YAŞAR contributed to all stages of the study, including conceptualization, research, methodology, writing-original draft, modeling and analysis.

REFERENCES

1. Adam, N. M., Attia, O. H., Al-Sulttani, A. O., Mahmood, H. A., As'arry, A. and Md Rezali, K. A. (2020). Numerical analysis for solar panel subjected with an external force to overcome adhesive force in desert areas. *CFDL,* 12(9), 60–75. doi: 10.37934/ cfdl.12.9.6075

2. Akula, R., Minnikanti, A. and Balaji, C. (2024). Pin fin-PCM composite heat sink solution for thermal management of cylindrical Li-ion battery, *Applied Thermal Engineering*, 248 (12), 123146. doi: 10.1016/j.applthermaleng.2024.123146

3. Aljumaili, A., Alaiwi, Y. and Al-Khafaji, Z. (2024). Investigating back surface cooling system using phase change materials and heatsink on photovoltaic performance, *Journal of Engineering and Sustainable Development*, 28(3), 294–315. doi: 10.31272/jeasd.28.3.1

4. Alzwayi, A. and Paul, M. C. (2024). Effective battery pack cooling by controlling flow patterns with vertical and spiral fins, *Thermal Science and Engineering Progress*, 55(4), 102907. doi: 10.1016/j.tsep.2024.102907

5. Ansys. (2013). *ANSYS Meshing User's Guide*, pp. 724–746.

6. Aslan, E., Aydın, Y. and Yaşa, Y. (2022). Consideration of graphene material in PCM with aluminum fin structure for improving the battery cooling performance, *International Journal of Energy Research*, 46(8), 10758–1069. doi: 10.1002/er.7878

7. Bamrah, P., Chauhan, M. K. and Sikarwar, B. S. (2022). CFD analysis of battery thermal management system, *Journal of Physics: Conference Series*, 2178(1), 12035. doi: 10.1088/1742-6596/2178/1/012035

8. Bernardi, D., Pawlikowski, E. and Newman, J. (1984). General energy balance for battery systems, *Electrochemical Society Extended Abstracts*, 84(2), 164–165.

9. Bhave, M. A. and Taherian, H. (2014). Aerodynamics of intercity bus and its impact on CO_2 reductions, *Fourteenth Annual Early Career Technical Conference,* The University of Alabama, Alabama, 165-172. doi: 10.13140/2.1.1252.7046

10. Bhawna., Phogat, P., Shreya, S., Jha, R. and Singh, S. (2025). Advancements and challenges in lithium-ion and lithium-polymer batteries: Towards sustainable energy storage solutions, *Ionics*, 31(6), 5263–5289. doi: 10.1007/s11581-025-06309-x

11. Bo, L., Mahdi, J. M., Rahbari, A., Majdi, H. S., Xin, Y., Yaïci, W. and Talebizadehsardari, P. (2022). Twisted-fin parametric study to enhance the solidification performance of phase-change material in a shell-and-tube latent heat thermal energy storage system, *Journal of Computational Design and Engineering*, 9(6), 2297–2313. doi: 10.1093/jcde/qwac107

12. Chen, D., Jiang, J., Kim, G. H., Yang, C. and Pesaran, A. (2016). Comparison of different cooling methods for lithium ion battery cells. *Applied thermal engineering*, 94, 846-854. doi: 10.1016/j.applthermaleng.2015.10.015

13. Chen, K., Chen, Y., She, Y., Song, M., Wang, S. and Chen, L. (2020). Construction of effective symmetrical air-cooled system for battery thermal management, *Applied Thermal Engineering*, 166, 114679. doi: 10.1016/j.applthermaleng.2019.114679

14. Chen, K., Wu, W., Yuan, F., Chen, L. and Wang, S. (2019). Cooling efficiency improvement of air-cooled battery thermal management system through designing the flow pattern, *Energy*, 167, 781–790. doi: 10.1016/j.energy.2018.11.011

15. Cheng, L., Garg, A., Jishnu, A. K. and Gao, L. (2020). Surrogate based multi-objective design optimization of lithium-ion battery air-cooled system in electric vehicles, *Journal of Energy Storage*, 31(2), 101645. doi: 10.1016/j.est.2020.101645

16. Cho, S. H., Cha, M. Y., Kim, M., Sohn, Y. J., Yang, T. H. and Lee, W. Y. (2016). A feasibility study for a stratospheric long-endurance hybrid unmanned aerial vehicle using a regenerative fuel cell system, *Journal of Electrochemical Science and Technology*, 7(1), 41–51. doi: 10.5229/JECST.2016.7.1.41

17. Cui, Y., Gu, X., Xi, J., Zou, Y., Wang, Y., Ding, P. and Wang, X. (2025). Performance optimization of lithium-ion battery based on CFD numerical simulation and deep learning algorithm, *Journal of Energy Storage*, 127(6), 117156. doi: 10.1016/j.est.2025.117156

18. Dagdevir, T. and Ding, Y. (2024). Numerical investigation of battery thermal management by using helical fin and composite phase change material, *Journal of Energy Storage*, 75 (9), 109674. doi: 10.1016/j.est.2023.109674

19. Domalanta, M. R. B., and Paraggua, J. A. D. (2023). A multiphysics model simulating the electrochemical, thermal, and thermal runaway behaviors of lithium polymer battery. *Energies*, 16(6), 2642. doi: 10.3390/en16062642

20. Dönmez, E. and Bulut, E. (2024). Investigation of the effect of different design and flow parameters on battery cooling system performance, *Uludağ University Journal of Faculty of Engineering*, 29(3), 819–830. doi: 10.17482/uumfd.1570344

21. Emam, M. and Ahmed, M. (2018). Cooling concentrator photovoltaic systems using various configurations of phase-change material heat sinks, *Energy Conversion and Management*, 158, 298–314. doi: 10.1016/j.enconman.2017.12.077

22. ERCmarket Website, (2025). Access address: https://www.ercmarket.com/gens-ace-5100mah-80c-222v-6s1p-lipo-battery-pack-with-ec5-plug/ Access date: 08.07.2025.

23. Esmaeili, Z. and Khoshvaght-Aliabadi, M. (2023). Thermal management and temperature uniformity enhancement of cylindrical lithium-ion battery pack based on liquid cooling equipped with twisted tapes, *Journal of the Taiwan Institute of Chemical Engineers*, 148, 104671. doi: 10.1016/j.jtice.2023.104671

24. Fan, X., Meng, C., Yang, Y., Lin, J., Li, W., Zhao, Y., Xie, S. and Jiang, C. (2023). Numerical optimization of the cooling effect of a bionic fishbone channel liquid cooling plate for a large prismatic lithium-ion battery pack with high discharge rate, *Journal of Energy Storage*, 72, 108239. doi: 10.1016/j.est.2023.108239

25. Fu, L., Zhang, Z., Sheng, L., Kuang, Z., Zhu, Z. and Bi, Q. (2025). Pouch lithium-ion battery thermal management by using a new liquid-cooling plate with honeycomb-like fins, *Case Studies in Thermal Engineering*, 69(367), 105945. doi: 10.1016/j.csite.2025.105945

26. Ghalambaz, M., Mahdi, J. M., Shafaghat, A., Eisapour, A. H., Younis, O., Sardari, P. T. and Yaïci, W. (2021). Effect of twisted fin array in a triple-tube latent heat storage system during the charging mode, *Sustainability*, 13(5), 2685. doi: 10.3390/su13052685

27. Hasan, H. A., Togun, H., Abed, A. M., Qasem, N. A. A., Abderrahmane, A., Guedri, K. and Eldin. S. M. (2023). Numerical investigation on cooling cylindrical lithium-ion-battery by using different types of nanofluids in an innovative cooling system, *Case Studies in Thermal Engineering*, 49 (January 1995), 103097. doi: 10.1016/j.csite.2023.103097

28. Incropera, F. P. and DeWitt, D. P. (1996). *Introduction to Heat Transfer*, John Wiley & Sons Inc, New York.

29. Ismail, M., Panter, J. R. and Landini, S. (2025). Numerical investigation of fin geometries on the effectiveness of passive, phase-change material− based thermal management systems for lithium-ion batteries. *Applied Thermal Engineering*, 262, 125216. doi: 10.1016/j.applthermaleng.2024.125216

30. Ji, S., Huadan, C., Qi, P., Liu, Z. and Li, P. (2025). Hydrothermal performance enhancement of heat sink using low flow-drag twisted blade-like fins. *International Journal of Heat and Fluid Flow*, 111, 109669. doi: 10.1016/j.ijheatfluidflow.2024.109669

31. Kim, C., Han, J. and Hong, S. (2022). Evaluation of spoiler model based on air cooling on lithium-ion battery pack temperature uniformity, *Processes*, 10(3), 505. doi: 10.3390/pr10030505

32. Kummitha, O. R. (2023). Thermal cooling of li-ion cylindrical cells battery module with baffles arrangement for airflow cooling numerical analysis, *Journal of Energy Storage*, 59 (2), 106474. doi: 10.1016/j.est.2022.106474

33. Larrañaga-Ezeiza, M.., Navarro, G. V., Garmendia, I. G., Arroiabe, P. F., Martinez-Aguirre, M. and Arostegui, J. B. (2022). Parametric optimisation of a direct liquid cooling–based prototype for electric vehicles focused on pouch-type battery cells, *World Electric Vehicle Journal*, 13(8), 149. doi: 10.3390/wevj13080149

34. Li, N., Liu, X., Yu, B., Li, L., Xu, J. and Tan, Q. (2021). Study on the environmental adaptability of lithium-ion battery powered UAV under extreme temperature conditions, *Energy*, 219(18), 119481. doi: 10.1016/j.energy.2020.119481

35. Li, X., He, F. and Ma, L. (2013). Thermal management of cylindrical batteries investigated using wind tunnel testing and computational fluid dynamics simulation, *Journal of Power Sources*, 238, 395–402. doi: 10.1016/j.jpowsour.2013.04.073

36. Li, Y. and Liu, M. (2022). Path planning of electric VTOL UAV considering minimum energy consumption in urban areas, *Sustainability*, 14(20), 13421. doi: 10.3390/su142013421

37. Li, Y., Zhang, K. and Chang, S. M. (2024). Optimization of fin parameters in cooling systems for temperature uniformity enhancement in battery module applications with offset strip fins, *Numerical Heat Transfer, Part A: Applications*, 86(16), 5648–5665. doi: 10.1080/10407782.2024.2333043

38. Liu, H., Jin, C., Li, H. and Ji, Y. (2023). A numerical study of PCM battery thermal management performance enhancement with fin structures, *Energy Reports*, 9, 1793–1802. doi: 10.1016/j.egyr.2023.04.214

39. Liu, J., Ma, Q. and Li, X. (2022). Numerical simulation of the combination of novel spiral fin and phase change material for cylindrical lithium-ion batteries in passive thermal management, *Energies*, 15(23), 8847. doi: 10.3390/en15238847

40. Luo, M., Zhang, Y., Wang, Z., Niu, Y., Lu, B., Zhu, J., Zhang. J. and Wang. K. (2024). Thermal performance enhancement with snowflake fins and liquid cooling in PCM-based battery thermal management system at high ambient temperature and high discharge rate, *Journal of Energy Storage*, 90(2), 111754. doi: 10.1016/j.est.2024.111754

41. Lv, Z., Sun, Z., Wang, L., Liu, Q. and Zhang, J. (2025). Multi-level thermal modeling and management of battery energy storage systems, *Batteries*, 11(6), 219. doi: 10.3390/batteries11060219

42. Mahamud, R. and Park, C. (2011). Reciprocating air flow for Li-ion battery thermal management to improve temperature uniformity. *Journal of Power Sources*, 196(13), 5685-5696. doi: 10.1016/j.jpowsour.2011.02.076

43. Murthy, K. K., Podila, A., Nataraj, C., Niranjan, H., Alagirisamy, M., Lakshmanan, R. and Selvaperumal, S. (2024). Enhancement of Heat Transfer in Octagonal Fin Tube Heat Exchanger with Various Side Ratios. In International Conference on Data Engineering and Communication Technology, 465-476. Springer Nature, Singapore. doi: 10.1007/978-981-96-5214-3_37

44. Pan, H., Liu, X., Yang, Q., Xu, H. and Xu, D. (2023). Three-dimensional Lattice Boltzmann study on structure optimization and heat dissipation performance of pin-fin heat sink integrated with phase change material, *Journal of Energy Storage*, 71(20), 108233. doi: 10.1016 /j.est.2023.108233

45. Patil, M. S., Seo, J. H., Panchal, S., Jee, S. W. and Lee, M. Y. (2020). Investigation on thermal performance of water-cooled Li-ion pouch cell and pack at high discharge rate with U-turn type microchannel cold plate, *International Journal of Heat and Mass Transfer*, 155 (04), 119728. doi: 10.1016/j.ijheatmasstransfer.2020.119728

46. Perini, F., Zha, K., Busch, S. and Reitz, R. (2017). Comparison of linear, non-linear and generalized RNG-based k-epsilon models for turbulent diesel engine flows, *SAE International*, doi: 10.4271/2017-01-0561

47. Schimpe, M., von Kuepach, M. E., Naumann, M., Hesse, H. C., Smith, K. and Jossen, A. (2018). Comprehensive modeling of temperature-dependent degradation mechanisms in lithium iron phosphate batteries, *Journal of the Electrochemical Society*, 165(2), A181–A193. doi: 10.1149/2.1181714jes

48. Sharma, A. R., Sai, C. S., Kumar, A., Reddy, R. V. J., Danyharsha, D. and Jilte, R. (2021). Three-dimensional CFD study on heat dissipation in cylindrical lithium-ion battery module, *Materials Today: Proceedings*, 46(9), 10964–10968. doi: 10.1016/j.matpr.2021.02.041

49. Shi, Q., Liu, Q., Zhang, B., Yao, X., Zhu, X., Ju, X. and Xu, C. (2025). Multi-objective optimization of an immersion cooling battery module with manifold jet impingement: Based on precision model for high-capacity batteries, *International Communications in Heat and Mass Transfer*, 161, 108448. doi: 10.1016/j.icheatmasstransfer.2024.108448

50. Shukla, I., Tupkari, S. S., Raman, A. K. and Mullick, A. N. (2012). Wall Y+ approach for dealing with turbulent flow through a constant area duct, *The 4th Internatonal Meeting of Advances in Thermofluids*, AIP Conference Proceedings, Melaka, 1395–1404. doi: 10.1063/1.4704213

51. Sissenwine, N., Wexler, H., Teweles, S. and Dubin, M. COESA. (1976). The United States Committee on Extension to the Standard Atmosphere.

52. Sklavounos, S. and Rigas, F. (2006). Simulation of Coyote series trials-Part I, *Chemical Engineering Science*, 61(5), 1434–1443. doi: 10.1016/j.ces.2005.08.042

53. Sun, X., Mahdi, J. M., Mohammed, H. I., Majdi, H. S., Zixiong, W. and Talebizadehsardari, P. (2021). Solidification enhancement in a triple-tube latent heat energy storage system using twisted fins, *Energies*, 14(21), 7179. doi: 10.3390/en14217179

54. Sutheesh, P. M., Atul, A. P. and Rohinikumar, B. (2024). Numerical and experimental investigations of thermal performance of lithium-ion battery with hybrid cooling system under dry-out condition, *Journal of Energy Storage*, 84, 110889. doi: 10.1016/j.est.2024.110889

55. Şefkat, G. and Özel, M. A. (2020). Elektrikli araçlarda kullanılan pil hücresinin elektriksel ve termal modeli, *Uludağ University Journal of The Faculty of Engineering*, 25(1), 51–64. doi: 10.17482/uumfd.541391

56. Tan, W. J., Kueh, T. C., Tan, M. K., Wang, X. and Hung, Y. M. (2025). Enhanced cooling performance of lithium polymer batteries using micro heat pipes integrated with carbon nanotubes coatings, *International Journal of Heat and Mass Transfer*, 247(49), 127164. doi: 10.1016/j.ijheatmasstransfer.2025.127164

57. Uzal, H., Şener, R. and Oktay, H. (2023). Elektrikli araçlarda hava giriş konumu ve hızının batarya soğutma performansına etkisinin araştırılması, *International Journal of Advances in Engineering and Pure Sciences*, 35(1), 116–124. doi: 10.7240/jeps.1239910

58. Vashisht, S., Rakshit, D., Panchal, S., Fowler, M. and Fraser, R. (2025). Experimental estimation of heat generating parameters for battery module using inverse prediction method, *International Communications in Heat and Mass Transfer*, 162 (100381), 108539. doi: 10.1016/j.icheatmasstransfer.2024.108539

59. Wang, F., Bai, L., Fletcher, J., Whiteford, J. and Cullen, D. (2008). Development of small domestic wind turbine with scoop and prediction of its annual power output, *Renewable Energy*, 33(7), 1637–1651. doi: 10.1016/j.renene.2007.08.008

60. Wang, H., He, F. and Ma, L. (2016). Experimental and modeling study of controller-based thermal management of battery modules under dynamic loads, *International Journal of Heat and Mass Transfer*, 103(9), 154–164. doi: 10.1016/j.ijheatmasstransfer.2016.07.041

61. Wang, J., Huang, W., Pei, A., Li, Y., Shi, F., Yu, X. and Cui. Y. (2019). Improving cyclability of Li metal batteries at elevated temperatures and its origin revealed by cryo-electron microscopy, *Nature Energy*, 4(8), 664–670. doi: 10.1038/s41560-019-0413-3

62. Wang, Z., Zou, Z., Zhou, Y., Geng, X., Sun, Y., Huang, X. and Hao, M. (2025). Performance comparison of battery cold plates designed using topology optimization across laminar and turbulent flow regime, *International Journal of Heat and Mass Transfer*, 238(1), 126450. doi: 10.1016/j.ijheatmasstransfer.2024.126450

63. Xiao, J., Zhang, X., Bénard, P., Yang, T., Zeng, J. and Long, X. (2023). Fin structure and liquid cooling to enhance heat transfer of composite phase change materials in battery thermal management system, *Energy Storage*, 5(6), doi: 10.1002/est2.453

64. Xiong, M., Wang, N., Li, W., Garg, A. and Gao, L. (2023). Study on the heat dissipation performance of a liquid cooling battery pack with different pin-fins, *Batteries*, 9(1), 44. doi: 10.3390/batteries9010044

65. Yakhot, V., Orszag, S. A., Thangam, S., Gatski, T. B. and Speziale, C. G. (1992). Development of turbulence models for shear flows by a double expansion technique, *Physics of Fluids A: Fluid Dynamics*, 4(7), 1510–1520. doi: 10.1063/1.858424

66. Yousefi, E., Ramasamy, D., Kadirgama, K., Talele, V., Najafi, H., Olyaei, M., Miljkovic, N. and Panchal, S. (2025). Electrochemical-thermal modeling of phase change material battery thermal management systems: Investigating mesh types for accurate simulations, *International Journal of Heat and Mass Transfer*, 247, 127107. doi: 10.1016/j.ijheatmasstransfer.2025.127107

67. Zhang, F., Wang, Y., Li, X., Tian, Z. and Xie, Y. (2025). Thermal characteristics and optimization of a novel liquid cooling plate with cavities and flow-enhancing fins, *International Communications in Heat and Mass Transfer*, 165(6), 109042. doi: 10.1016/j.icheatmasstransfer.2025.109042

68. Zhao, G., Wang, X., Negnevitsky, M., Li, C., Zhang, H. and Cheng, Y. (2023). A high-performance vortex adjustment design for an air-cooling battery thermal management system in electric vehicles, *Batteries*, 9(4), 208. doi: 10.3390/batteries9040208

69. Zolot, M., Pesaran, A. A. and Mihalic, M. (2002). Thermal evaluation of Toyota Prius battery pack, *SAE International*, doi: 10.4271/2002-01-1962